Coupling between a laser and a prestructured target with an arbitrary structure period

K. Q. Pan,[1] S. E. Jiang,[1,*] L. Guo,[1] S. W. Li,[1] Z. C. Li,[1] D. Yang,[1,†] C. Y. Zheng,[2,3] B. H. Zhang,[1] and X. T. He[2,3]

[1]*Laser Fusion Research Center, China Academy of Engineering Physics, Mianyang 621900, China*

[2]*Center for Applied Physics and Technology, Peking University, Beijing 100871, China*

[3]*Institute of Applied Physics and Computational Mathematics, Beijing 100088, China*

(Received 28 June 2018; published 1 November 2018)

The coupling between a laser and a prestructured target with an arbitrary structure period is investigated with the help of two-dimensional (2D) particle-in-cell (PIC) simulations. It is shown that new electromagnetic (e.m.) waves will be generated after the coupling. Since the coupling is a resonant process, strong surface currents will be generated, which result in the generation of strong quasistatic magnetic fields. The frequencies which the newly excited e.m. waves contain are harmonics of the laser frequency and the frequencies can be controlled by the structure period. Also, the propagation directions of the newly excited e.m. waves are well controlled by the ratio between the structure period and the laser wavelength, which means e.m. waves excited by lasers with different frequencies have different propagation directions. As a result, the prestructured target can act as a new kind of optical gratings which can be used to split superintense laser pulses. The controlling of both the harmonic frequencies and the propagation directions can be explained by matching condition of the coupling, which is a formula resembling but physically different from the diffraction grating equation. The quasistatic magnetic fields are on the target front surface and as strong as hundreds of teslas, but the amplitude will be decreased by the newly excited e.m. waves when they are propagating along the target surface. Since the propagation directions are controlled by the structure period, with an optimal structure period, the prestructured target can also act as a source of strong quasistatic magnetic fields.

DOI: 10.1103/PhysRevE.98.053201

I. INTRODUCTION

Lasers-solid interactions have been hot topics because of their wide applications, such as charged particles acceleration [1–5] and radiation generation [6–13]. However, it is well known that a laser will only penetrate into the skin depth of a solid target, so energy conversion from the laser to hot electrons is usually low. People are sparing no efforts to find out ways of improving the energy conversion efficiency of the laser-solid interactions. Among these efficient ways, microstructure on the target surface is one of the best choices. For example, subwavelength microstructure is used in laser-driven electron heating, it is shown that the energy conversion efficiency from the laser to hot electrons is more than 90% [14–16]. Besides, people also use nanoscale microstructures to improve the quality of the accelerated electrons [17,18]. It is shown that, when there are microstructures on the target back surface, the accelerated electrons will be well guided by the nanoscale microstructures. When the scale of the microstructure is in the wavelength scale, it is widely used to generate the surface plasma waves (SPWs) [18–23]. It is shown that the excitation of the SPWs alsohas many applications. Besides enhancing the electron heating [19], the excitation of the SPWs may also enhance the ion acceleration [20], the synchrotron radiation [10] and quasistatic magnetic field generation [21,22]. It is also reported both numerically and experimentally that the excitation of the SPWs can be used as a source of high-order harmonics [24–26]. However, people paid more attention to the charged particles acceleration and the radiation generation when they investigated the interaction between a laser and a prestructured target. And the coupling mechanism between a laser and a prestructured target with an arbitrary structure period has not been systematically investigated until now. As a result, for better applications, it is necessary to further study the coupling mechanism between a laser and a prestructured target with an arbitrary structure period.

In this paper, with the help of two-dimensional (2D) particle-in-cell (PIC) simulations, we investigate the coupling between a laser and a prestructured target with an arbitrary structure period. The prestructured target is shown in Fig. 1. We find that both new electromagnetic (e.m.) waves and quasistatic magnetic fields are generated after the coupling. However, the newly excited e.m. waves are not definitely propagating along the target surface, instead, the propagation direction are governed by the ratio λ_0/λ_s, where λ_0 and λ_s are the laser wavelength and the structure period, respectively. The angle between the target surface and propagation direction is $\theta = \cos^{-1}(\lambda_0/\lambda_s)$. We also find that the amplitude of the quasistatic magnetic field is strongly influenced by the newly excited e.m. waves, when these e.m. waves are propagating along the target surface, the strength of the quasistatic magnetic field will be decreased. We also discuss the influence of the structure period on the electron heating. It is shown that transverse momentum is strongly influenced, but not the electron energy spectrum.

*jiangshn@vip.sina.com

†yangdong.caep@gmail.com

The paper is arranged as follows. In Sec. II we discuss the newly generated e.m. waves which contain high-order harmonics. In Sec. III we discuss the influences of the target period on quasistatic magnetic field generation and electron heating. The last two sections are the conclusion and the acknowledgments.

II. ELECTROMAGNETIC WAVES GENERATED BY THE COUPLING BETWEEN THE LASER AND THE PRESTRUCTURED TARGET

To study the coupling mechanism between the laser and the prestructured targets, we perform four 2D PIC simulations with EPOCH code [27]. The geometry of the prestructured targets is shown in Fig. 1. The target is located in the x-y plane, the p-polarized Gaussian laser pulse is propagating in the x direction with the electric field E_y and the sinusoidal target structure is periodically distributed along the y axis with the depth λ_0. In the simulations, the simulation box is $30\lambda_0 \times 40\lambda_0$ in the $x \times y$ directions and the grid step of the simulation box is $0.01\lambda_0 \times 0.01\lambda_0$. The plasma is located in $x/\lambda_0 > 20$ and $-20 < y/\lambda_0 < 20$, its density is $n_e = 50n_c$ [such a low density is used to make sure that the grid step is smaller than the skin depth of the laser $l_s = c/\omega_{pe}$, where $\omega_{pe} = \sqrt{4\pi n_e e^2/m_e}$ is the plasma frequency, however, the simulation results change little with higher plasma density $(900n_c)$], where $n_c = m_e\omega_0^2/4\pi e^2$ is the laser critical density; m_e and e are the electron mass and charge, respectively; and ω_0 is the laser frequency. Because the laser prepulse is usually intense enough to fully ionize the target before the main pulse arrives, the plasmas in the simulation are initially fully ionized. The collisional effects are not considered in the simulation, because the plasma is hot and the collisional effects are negligible. To make sure that the target structure is not damaged much, the laser intensity is not too high and the pulse duration is also not too long. The normalized vector potential of the Gaussian laser is $a_0 = eE_0/m_e\omega_0 c = 3$, where E_0 is the laser peak electric field and c is the light speed. And the laser duration is $\tau = 40T_0$, where $T_0 = 2\pi/\omega_0$ is the laser period. And the transverse profile of the laser is e^{-y^2/r_0^2}, where $r_0 = 5\lambda_0$ is the laser beam radius. This beam radius makes sure that there are at least five structure peaks in the beam radius. In the four simulations, we randomly choose four structure periods, which are λ_0, $\sqrt{2}\lambda_0$, $1.5\lambda_0$, and $2\lambda_0$. The simulation results are shown in Figs. 2–7.

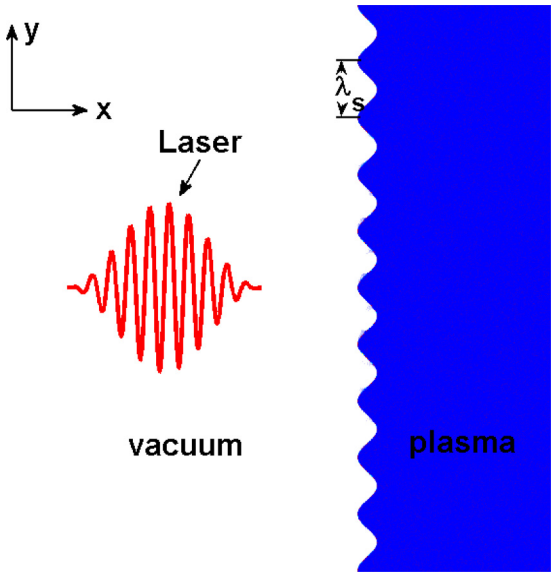

FIG. 1. Geometry of laser interaction with prestructured target. The p-polarized laser is propagating in the x direction and its electric field lies in the y direction. The structure is periodically distributed along the y axis and is uniform along the z axis.

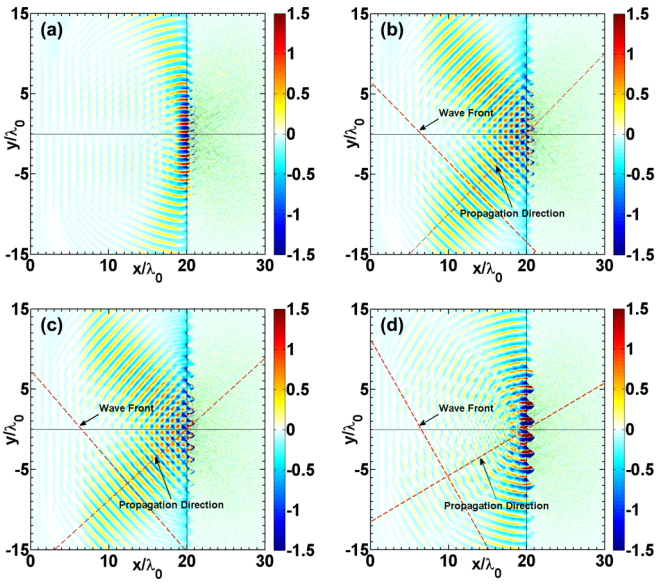

FIG. 2. Snapshots of the longitudinal electric field E_x for four different structure periods at $t = 38T_0$. (a) $\lambda_s = \lambda_0$, (b) $\lambda_s = \sqrt{2}\lambda_0$, (c) $\lambda_s = 1.5\lambda_0$, and (d) $\lambda_s = 2\lambda_0$. The electric field is normalized by $m_e\omega_0 c/e$.

Figure 2 shows the snapshots of the electric fields E_x for the four cases at $t = 38T_0$. In Fig. 2(a), the structure period is $\lambda_s = \lambda_0$. Figure 2(a) shows that, the newly generated e.m. waves are propagating along the target surface, these e.m. waves are the so-called surface plasma waves as discussed in our previous works [26,28]. In Fig. 2(b), the structure period is $\lambda_s = \sqrt{2}\lambda_0$, we find that the newly excited e.m. waves are no longer propagating along the target surface, as shown in Fig. 2(c), where the structure period is $\lambda_s = 1.5\lambda_0$. The angles between the target surface and the propagation directions of these two cases are 45° and 48.5°, respectively. The cosines of these two angles are just $1/\sqrt{2}$ and $2/3$, respectively. In Fig. 2(d), the structure period is $\lambda_s = 2\lambda_0$, for this case, the newly excited e.m. waves have four propagation directions, two of them are along the target surface (the SPW)and the angle between the other two and the target surface is 60°, whose cosine is just $1/2$. To conclude for Fig. 2, new e.m. waves will be excited after the coupling between the laser and the prestructured target, and the angle between the target surface and the propagation directions of the newly excited e.m. waves is $\theta = \cos^{-1}(\lambda_0/\lambda_s)$, which is also valid for the SPWs whose $\theta \approx 0$ and the reflected light from a flat target $(\lambda_s = \infty)$ whose $\theta = 90°$.

To explain the results shown in Fig. 2, we need to discuss the wave equations of the newly excited e.m. waves. To exclude the driven laser, we only discuss the E_x component, the wave equation is

$$\frac{1}{c^2}\frac{\partial^2 E_x}{\partial t^2} - \nabla^2 E_x = -\mu_0 \frac{\partial j_x}{\partial t}. \quad (1)$$

In Eq. (1), the source current is $j_x = -e\delta n_e u_x$, where δn_e is the electron density perturbation, u_x is the fluid velocity of the electrons (the motion of the ions is neglected). Then the Fourier transform of Eq. (1) is $(\omega^2 - c^2k^2)E_x(\omega, \mathbf{k}) = -iec^2\mu_0\omega\delta n_e(\omega_n, \mathbf{k}_n)u_x(\omega_u, \mathbf{k}_u)$, and the resonance conditions are $\mathbf{k} = \mathbf{k}_u + \mathbf{k}_n$ and $\omega = \omega_n + \omega_u$. Since the only driver of j_x is the laser, the frequencies E_x possesses should be harmonics of ω_0, i.e., $\omega = n\omega_0$ $(n = 1, 2, 3, \dots)$. For simplification, we only discuss $\omega = \omega_0$, for example, and then we have $k = \omega_0/c$. As is discussed in our previous work [26,28], the wave numbers of the electron density perturbation $\delta n_e(\omega_n, \mathbf{k}_n)$ is governed by the structure period λ_s, which is $\mathbf{k}_n = m(\lambda_0/\lambda_s)\omega_0/c\hat{\mathbf{y}}$ (where $m = \pm1, \pm2, \pm3, \dots$ and $\hat{\mathbf{y}}$ is the direction of the y axis). Again we discuss the lowest order $m = 1$, i.e., $k_n = (\lambda_0/\lambda_s)\omega_0/c$. Since u_x is oscillating in the x direction, we could say that $\mathbf{k}_u$ is only in the x direction. Then from the wave-number matching condition, we have $k_y = k\cos\theta = k_n = (\lambda_0/\lambda_s)\omega_0/c$, where θ is the angle between the target surface and propagation direction $\mathbf{k}$. In other words, we have $\cos\theta = \lambda_0/\lambda_s$. This formula is also valid for the nth-order harmonic only if $|m| = n$. For the case $\lambda_s = 2\lambda_0$, if $|m| = 2n$, then $\cos\theta = m\lambda_0/(n\lambda_s) = \pm1$ is satisfied, so we also observe SPWs which are propagating along the target surface in Fig. 2(d). However, for cases $\lambda_s = \sqrt{2}\lambda_0$ and $\lambda_s = 1.5\lambda_0$, if $m \geqslant 2n$, we have $\cos\theta > 1$, no θ will meet the expression, so we find no SPWs in Figs. 2(b) and 2(c).

To further prove the validity of the above discussion, in Fig. 3, we give the wave-number spectra of the fields shown in Fig. 2. It is shown that, for the propagation directions of these newly excited e.m. waves, Fig. 3 gives the same results as Fig. 2. Besides, Fig. 3 also shows that the newly excited waves contain high-order harmonics, which just shows the validity of the above analysis. It is also necessary to point out that, the SPWs shown in Fig. 3(d) seem to contain half integer order harmonics, which is also corresponding to the formula $k_n = m(\lambda_0/\lambda_s)\omega_0/c$(here, $m = 1, 3, 5, \dots$). However, as is pointed out in our previous works that these modes are not moving e.m. waves, because their frequencies are also harmonics of ω_0 and the dispersion relation of the e.m. wave $\omega = ck$ can't be satisfied. It's more likely that they are standing waves trapped in the structure and periodically distributed along the y axis. This phenomenon also proves the validity of the discussion of Fig. 2(d), i.e., when $|m| = 2n$ is satisfied, SPWs will be generated. The same explanation is also valid for the modes (standing waves) observed on the k_y axes of Figs. 3(b) and 3(c), we find no SPWs propagating along the target surface in Figs. 2(b) and 2(c). Now suppose a two-color laser is irradiating on such a prestructured target, it is easy to judge for the formula $\cos\theta = \lambda_0/\lambda_s$ that the newly excited e.m. waves excited by the two colors have different propagation directions, so this kind of prestructured targets can be well used as optical gratings that can split a superintense laser with several colors. However, if the intensity of the light (such as the natural light) is so low that a solid target cannot even be ionized into plasma, this grating will no longer work.

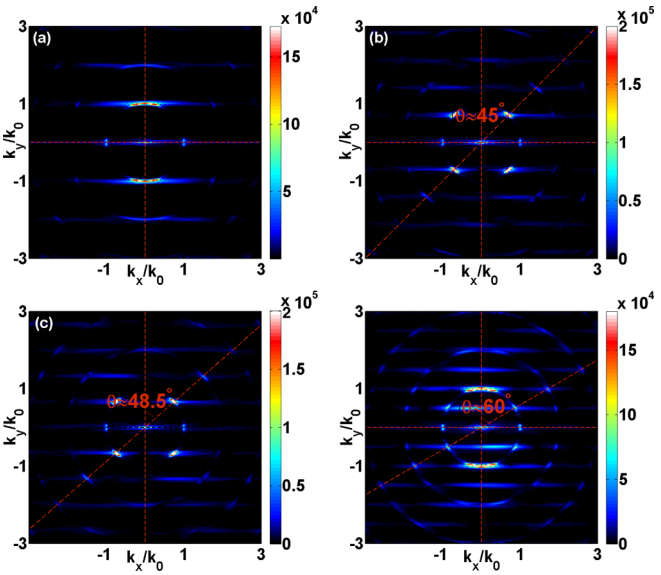

FIG. 3. Wave-number spectra of the electric fields shown in Fig. 2. The colorbar is in an arbitrary unit. In this figure, the red dashed lines in the transverse direction mark the directions of the target surfaces, the red dashed lines in the longitudinal direction mark the directions of the target normal and the red dashed lines in the oblique directions mark the propagation directions of the newly generated e.m. waves. And the noted angles are the angles between the target surfaces and the propagations directions of the newly generated e.m. waves.

Since the prestructured target, which can also act as a traditional optical grating, can be used as a plasma optical grating that can split superintense lasers, it is necessary to discuss the differences between the traditional optical grating and our plasma optical grating. As is known that the diffraction grating equation of a traditional optical grating is $d|\sin\theta_i \pm \sin\theta_j| = j\lambda$, where d is the period of the grating, λ is the laser wavelength, j is the order of the diffracted light, θ_i is the laser incident angle and θ_j is the diffraction angle which describes the angle between the target normal and the observation direction. Noting that the incident angles considered in this paper is $\theta_i = 0$, $d = \lambda_s$ and the diffracted angle is actually the complementary angle of the angle θ, we find that the grating equation becomes $\cos\theta = j\lambda_0/\lambda_s$. When the first diffraction order ($j = 1$) is considered, it is amazing to find that the diffraction equation also becomes $\cos\theta = \lambda_0/\lambda_s$. From the analysis of Fig. 2(d), we find that the matching condition of the generation of newly excited e.m. waves also becomes $\cos\theta = m\lambda_0/\lambda_s$, which is also similar to the diffraction equation. However,the plasma grating discussed in this paper is totally different from the traditional optical grating. First, one needs a convex lens to observe the strengthened diffracted lights of a parallel light beam, however, the newly excited e.m. waves need not. Second, the integer number j in the diffraction equation is the diffraction order which describes the strength of the diffracted lights, but the number m for our matching condition is the wave-number harmonic order of the electron density perturbation. Third,

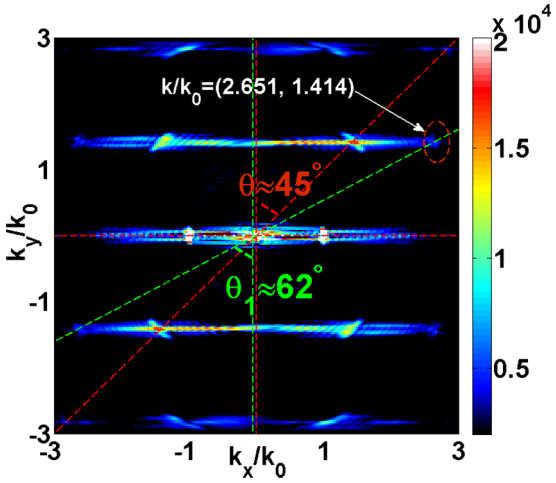

FIG. 4. Wave-number spectrum of E_x of the case $\lambda_s = \lambda_0/\sqrt{2}$. In this figure, the dashed lines are plotted for the same purpose as Fig. 3.

the more accurate matching condition is actually $\cos\theta = m\lambda_0/(n\lambda_s)$, where n is the frequency harmonic order of the newly excited e.m. waves. For example, when $\lambda_s = \lambda_0/\sqrt{2}$, we have $\cos\theta = \sqrt{2}m/n < 1$. Since m and n are all integer numbers, we have $n \geqslant 2m$. Take $n = 2m$ for example, we have $\theta = 45^\circ$, i.e., in the direction $\theta = 45^\circ$, new e.m. waves will be excited. However, it is also necessary to point out that the minimum n is $n_{\min} = 2$, in other words, the lowest harmonic of the newly excited e.m. wave is the second. As a result, we can also conclude that the frequencies of the newly excited e.m. waves is also controlled by the structure period. The case $\lambda_s = \lambda_0/\sqrt{2}$ is also simulated by a 2D PIC simulation and the wave-number spectrum of E_x is given in Fig. 4. Figure 4 shows that the simulation result agrees well with the theoretical analysis. The figure also proves the validity of the case $n = 3m$, in which $n_{\min} = 3$ and $\theta \approx 62^\circ \approx \cos^{-1}(\sqrt{2}/3)$ [the angle between the two dashed green lines in Fig. 4, i.e., $\tan^{-1}(2.651/1.414)$].

III. INFLUENCE OF THE STRUCTURE PERIOD TO THE QUASISTATIC MAGNETIC FIELD GENERATION AND ELECTRON HEATING

After discussing the coupling mechanism between the laser and the prestructured target, we will continue to discuss the influence of the structure period on the quasistatic magnetic field generation and electron heating. The influence of the structure period on the quasistatic magnetic field generation is shown in Fig. 5, which shows the snapshots of the quasistatic (averaged on several laser cycles) magnetic fields B_z for the four cases at $t = 38T_0$. It is obviously shown that, in the area the laser irradiates ($-5 < y/\lambda_0 < 5$, we call it the source area), the structure of the magnetic fields is different from that out of this area. From Fig. 2 we know that this area is actually the origin of the newly excited e.m. waves. In this area, two newly excited e.m. waves with two different propagation directions will meet each other to generate standing waves. When the electrons are trapped in the wave node, it will generate magnetic fields with the structure(dipole)

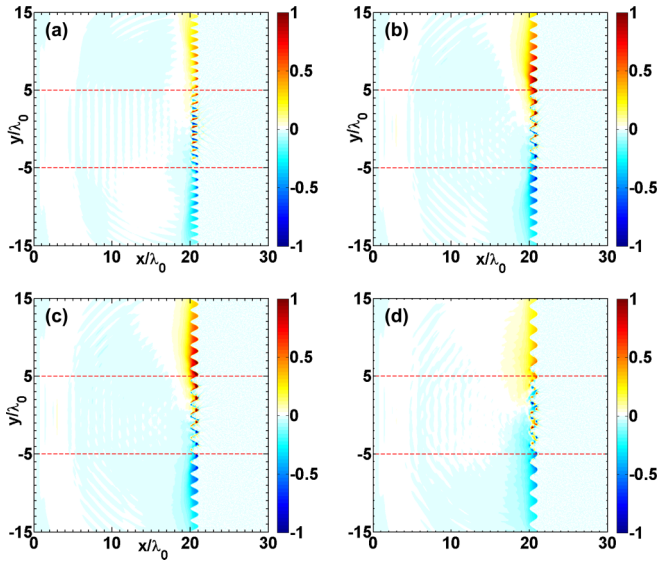

FIG. 5. Snapshots of the quasistatic magnetic field $\bar{B}_x$ for the four structure periods at $t = 38T_0$. The magnetic field is achieved by averaging the magnetic field B_x within three laser cycles. And the magnetic field is normalized by $m_e\omega_0/e$.

shown in the source area [Fig. 5(a) is more clear]. As to the quasistatic magnetic fields out of the source area, it is shown from Fig. 5 that, when the SPWs are excited, the intensity of the quasistatic magnetic fields will be decreased. To explain the decrease of the quasistatic magnetic fields, we plot the phase spaces $p_y - y$ of the electrons out of the source area for the four cases, as is shown in Fig. 6.

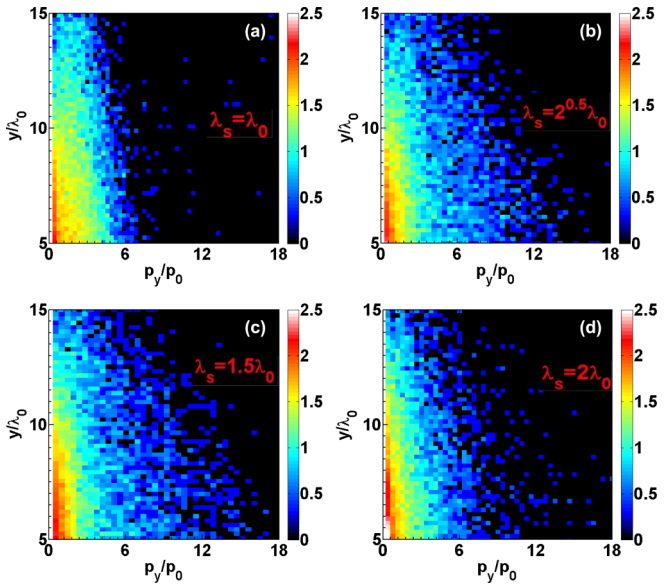

FIG. 6. Snapshots of the phase spaces $y - p_y$ for the four structure periods at $t = 38T_0$. The four structure periods are $\lambda_s = \lambda_0$ (a), $\lambda_s = \sqrt{2}\lambda_0$ (b), $\lambda_s = 1.5\lambda_0$ (c), and $\lambda_s = 2\lambda_0$ (d). The space is normalized by the laser wavelength λ_0 and the momentum is normalized by the electron momentum at light speed $m_e c$. The colorbar is the number of the electrons in logarithmic scale.

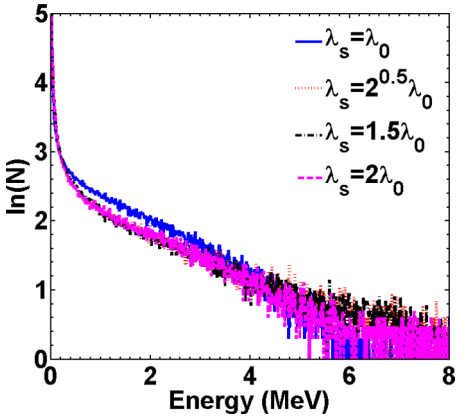

FIG. 7. Snapshots of the electron energy spectra for the four structure periods at $t = 38T_0$.

The generation of quasistatic magnetic fields on the surface of a prestructured target is regarded as a secondary effect of the SPW excitation in previous works [21,22]. However, the simulation results show that quasistatic magnetic fields will be generated even if the newly excited e.m. waves are not propagating along the target surface. As a result, in this paper, we owe the generation of the quasistatic magnetic fields to the generation of a steady surface current, for the magnetic field B_z shown in Fig. 5 the current is $\bar{j}_y = -en_e p_y/\gamma$. So we give the phase spaces $p_y - y$ of the electrons out of the source area at $t = 38T_0$ in Fig. 6. It is obviously shown that, for the cases with no SPWs excitation, the electrons out of the source area have a larger maximum p_y and the number of the electrons with larger p_y is also larger, that is why the quasistatic magnetic fields out of the source area are more intense for the cases without SPWs excitation, as is seen in Fig. 5. It is also worth to be pointed out that all these electrons shown in Fig. 6 have positive p_y (however, in the area $y/\lambda_0 < -5$, electrons have only negative p_y, which is not shown here), which results in the quasistatic magnetic fields shown in Fig. 5. To explain how the SPWs influence p_y, we should know the origin of p_y. Although the electric field of the laser is E_y, the origin of p_y is not E_y because there is no laser out of the source area. As is known that a Gaussian laser pulse has a transverse ponderomotive force which tends to push the electrons to the wings of the laser, that's why the electrons in the area $y/\lambda_0 > 5$ tend to move up ($p_y > 0$) and the electrons in the area $y/\lambda_0 < -5$ tend to move down ($p_y < 0$). For the case of SPWs excitation, the standing wave in the source area is more intense, as is seen in Fig. 2, as a result, more electrons will be trapped in the node of the standing wave. After the electrons with higher energies overcome the barrier of the standing wave, the energy obtained from the ponderomotive force is also decayed. So what decreases the p_y and the number of hotter electrons for the cases with SPWs excitation is the standing wave of the SPWs in the source area.

In Fig. 7, we give the spectrum of the electron heating at $t = 38T_0$ for the four cases. It is shown that the excitation will also influence the electron heating. In the cases with SPWs excitation, the maximum electron energy is about 6 MeV, but in the cases without SPWs excitation, the maximum electron energy is about 8 MeV. The electron numbers in the energy range from 3 to 5 MeV are nearly the same for the four case. So we can conclude that the structure period actually has small influences on the electron heating.

IV. CONCLUSION

Simulations with other parameters are also performed to verify the robustness of our findings. The results will not be shown in this paper any more, but we will discuss them in this conclusion. First, we find that newly excited e.m. waves will still be excited even if there is a preplasma on the target surface. However, when the density scale length of the preplasma is too large ($> \lambda_0$), both the intensity distributions and the wave-number spectra of the newly excited e.m. waves become more complex because the laser will interact with the preplasma first. To avoid preplasmas with long density scale lengths, it is better to use a laser with higher contrast. Second, we find that the laser intensity ($a_0 < 30$) and the pulse duration ($\tau < 60T_0$) have little influences on the findings as long as the target structure is not damaged too much. However, the laser transverse profile will have some influences on the magnetic field generation, a gaussian profile is better for the magnetic fields generation. Third, we find that the shape of the target structure also has little influences on the findings. In these simulations, even if we use several structure shapes including the sinusoidal shape, the triangular shape, the rectangular shape and the grating, the simulation results related to the newly excited e.m. waves generation keep the same. We also find the the wavelength of the structure cannot be neither too large nor too small. From the formula $\cos\theta = m\lambda_0/(n\lambda_s)$ we know that $m\lambda_0/(n\lambda_s) \leqslant 1$. When λ_s/λ_0 is too large, the spectrum of the newly excited e.m. waves will be too complex because the parameter n will satisfy the inequality will many different values. However, when λ_s/λ_0 is too small, the minimum value of n (the order of the frequency harmonic) will become too large, in this case, the newly excited e.m. waves will be very weak or even cannot be excited.

In conclusion, we investigate the coupling between a laser and a prestructured target with an arbitrary structure period by 2D PIC simulations. The simulation results show that, when the laser is coupled to the prestructured targets, new e.m. waves will be resonantly excited. Since the coupling process is a resonant process, strong surface currents will be generated, which results in the generation of strong quasistatic magnetic fields. It is also shown that the propagation directions as well as the frequencies of the newly excited e.m. waves are well controlled by the structure period λ_s, the angle between the propagation direction and the target surface is $\theta = \cos^{-1}(m\lambda_0/n\lambda_s)$, which gives $m\lambda_0/n\lambda_s < 1$. Since $m\lambda_0/n\lambda_s < 1$, when $\lambda_s < \lambda_0$, n has a minimum value and the minimum n is the lowest order of the frequency harmonics, so the frequencies of the newly excited e.m. waves are also controlled by the structure period. The formula $\theta = \cos^{-1}(\lambda_0/\lambda_s)$ ($m = n = 1$) is also valid for the SPWs propagating along the target surface ($\lambda_s = \lambda_0$ or $\theta = 0$) and the reflected light from a plane target ($\lambda_s = \infty$ or $\theta = \pi/2$). Even if the formula quite resembles the diffraction grating equation, the two mechanisms should be distinguished for three reasons discussed in the last paragraph of Sec. II. Besides, the newly

excited e.m. waves possess high-order harmonics, which is also a property the diffracted lights never possess. When a laser with multicolors is coupled to the prestructured targets, it will generate e.m. waves propagating in different directions, so this kind of prestructured targets can be used as novel plasma optical gratings which can split superintense lasers. We also discuss the influence of the structure periods on the quasistatic magnetic field generation and electron heating. The generation of quasistatic magnetic fields on the surface of a prestructured target is regarded as a secondary effect of the SPW excitation in previous works [21,22], however, we find that even if the newly excited e.m. waves are not propagating, quasistatic magnetic fields are still generated. So we give a new explanation of the generation of the magnetic fields on the target surface, which owes the generation of the quasistatic magnetic fields to the generation of strong surface current. It is also shown that the quasistatic magnetic field out of the source area will be decreased by the standing wave of the SPWs, so we need to avoid the generation of SPWs when we want to generate stronger magnetic fields on the target surface. However, the electron heating is slightly influenced. So this work also gives a guidance for us to use a prestructured target to generate strong magnetic fields or enhance the electron heating.

ACKNOWLEDGMENTS

This research was supported by Science Challenge Project (Grant No. TZ2016005), China Postdoctoral Science Foundation (Grant No. 2017M620430), National Natural Science Foundation of China (Grants No. 11435011, No. 11575035, and No. 11705180) and the National Basic Research Program of China (Grant No. 2013CB834101).

[1] F. Brunel, Phys. Rev. Lett. **59**, 52 (1987).
[2] H. B. Cai, W. Yu, S. P. Zhu, and C. Y. Zheng, Phys. Plasmas **13**, 113105 (2006).
[3] B. Qiao, M. Zepf, M. Borghesi, and M. Geissler, Phys. Rev. Lett. **102**, 145002 (2009).
[4] X. Q. Yan, C. Lin, Z. M. Sheng, Z. Y. Guo, B. C. Liu, Y. R. Lu, J. X. Fang, and J. E. Chen, Phys. Rev. Lett. **100**, 135003 (2008).
[5] D. Wu, B. Qiao, C. McGuffey, X. T. He, and F. N. Beg, Phys. Plasmas **21**, 123118 (2014).
[6] L. L. Ji, A. Pukhov, E. N. Nerush, I. Yu. Kostyukov, B. F. Shen, and K. U. Akli, Phys. Plasmas **21**, 023109 (2014).
[7] R. Capdessus, E. d'Humières, and V. T. Tikhonchuk, Phys. Rev. Lett. **110**, 215003 (2013).
[8] C. P. Ridgers, C. S. Brady, R. Duclous, J. G. Kirk, K. Bennett, T. D. Arber, A. P. L. Robinson, and A. R. Bell, Phys. Rev. Lett. **108**, 165006 (2012).
[9] K. Q. Pan, C. Y. Zheng, Dong Wu, and X. T. He, Phys. Plasmas **22**, 083301 (2015).
[10] K. Q. Pan, C. Y. Zheng, D. Wu, L. H. Cao, Z. J. Liu, and X. T. He, Appl. Phys. Lett. **107**, 183902 (2015).
[11] F. Quéré, C. Thaury, P. Monot, S. Dobosz, Ph. Martin, J. P. Geindre, and P. Audebert, Phys. Rev. Lett. **96**, 125004 (2006).
[12] D. an der Brügge and A. Pukhov, Phys. Plasmas **17**, 033110 (2010).
[13] M. Yeung, B. Dromey, S. Cousens, T. Dzelzainis, D. Kiefer, J. Schreiber, J.H. Bin, W. Ma, C. Kreuzer, J. Meyer-ter-Vehn *et al.*, Phys. Rev. Lett. **112**, 123902 (2014).
[14] W. M. Wang, Z. M. Sheng, and J. Zhang, Phys. Plasmas **15**, 030702 (2008).
[15] M. M. Murnane and H. C. Kapteyn, Appl. Phys. Lett. **62**, 1068 (1993).
[16] G. Y. Hu, A. L. Lei, J. W. Wang, L. G. Huang, W. T. Wang, X. Wang, Y. Xu, B. F. Shen, J. Liu, W. Yu *et al.*, Phys. Plasmas **17**, 083102 (2010).
[17] L. Cao, Y. Gu, Z. Zhao, L. Cao, W. Huang, W. Zhou, H. B. Cai, X. T. He, Wei Yu, and M. Y. Yu, Phys. Plasmas **17**, 103106 (2010).
[18] Z. Zhao, L. Cao, L. Cao, J. Wang, W. Huang, W. Jiang, Y. He, Y. Wu, B. Zhu, K. Dong *et al.*, Phys. Plasmas **17**, 123108 (2010).
[19] M. Raynaud, J. Kupersztych, C. Riconda, J. C. Adam, and A. Héron, Phys. Plasmas **14**, 092702 (2007).
[20] T. Ceccotti, V. Floquet, A. Sgattoni, A. Bigongiari, O. Klimo, M. Raynaud, C. Riconda, A. Heron, F. Baffigi, L. Labate *et al.*, Phys. Rev. Lett. **111**, 185001 (2013).
[21] A. Bigongiari, M. Raynaud, and C. Riconda, Phys. Rev. E **84**, 015402(R) (2011).
[22] A. Bigongiari, M. Raynaud, C. Riconda, A. Héron, and A. Macchi, Phys. Plasmas **18**, 102701 (2011).
[23] P. K. Kaw and J. B. McBride, Phys. Fluids **13**, 1784 (1970).
[24] X. Lavocat-Dubuis and J.-P. Matte, Phys. Rev. E **80**, 055401(R) (2009).
[25] M. Cerchez, A. L. Giesecke, C. Peth, M. Toncian, B. Albertazzi, J. Fuchs, O. Willi, and T. Toncian, Phys. Rev. Lett. **110**, 065003 (2013).
[26] K. Q. Pan, C. Y. Zheng, and X. T. He, Phys. Plasmas **23**, 023109 (2016).
[27] C. S. Brady and T. D. Arber, Plasma Phys. Controlled Fusion **53**, 015001 (2011).
[28] K. Q. Pan, S. E. Jiang, S. W. Li, D. Yang, Z. C. Li, L. Guo, C. Y. Zheng, B. H. Zhang, and X. T. He, AIP Adv. **7**, 125215 (2017).